Continental Shelf Research 30 (2010) 1854–1864

Contents lists available at ScienceDirect

Continental Shelf Research

journal homepage: www.elsevier.com/locate/csr

Research papers

Tidal changes in estuarine systems induced by local geomorphologic modifications

Ana Picado [a], João M. Dias [a,*], André B. Fortunato [b]

[a] CESAM, Departamento de Física, Universidade de Aveiro, Campus de Santiago, 3810-193 Aveiro, Portugal
[b] LNEC—Laboratório Nacional de Engenharia Civil, Departamento de Hidráulica e Ambiente, Núcleo de Estuários e Zonas Costeiras, 1700-066 Lisboa, Portugal

ARTICLE INFO

Article history:
Received 19 April 2010
Received in revised form
25 August 2010
Accepted 26 August 2010
Available online 15 September 2010

Keywords:
Numerical model
Tidal currents
Tidal asymmetry
Tidal prism
Tidal changes
Ria de Aveiro

ABSTRACT

Although rising global sea levels will affect the estuarine flooded areas over the coming decades, the local and regional-scale processes will also induce important changes in these coastal systems. The main aim of this work is to investigate possible tidal changes in estuarine systems induced by local geomorphologic modifications, analysing the particular case of Ria de Aveiro which is in risk of inundation. Located in the Portuguese west coast, this tidally driven lagoon has a large area of mostly abandoned salt pans, which are in progressive degradation caused by the lack of maintenance and by the strong currents which erode their protective walls.

To explore possible tidal changes the hydrodynamic model ELCIRC was applied to Ria de Aveiro to simulate and analyse the impact in the lagoon hydrodynamics of this degradation which results in the enlargement of the lagoon flooded area. A high-resolution grid (grid spacing of the order of 1 m) was developed in order to represent the narrow channels adjacent to the salt pans. The hydrodynamic model was then successfully calibrated and assessed for skill for the Aveiro lagoon through comparison between measurements and model results and quantification of the numerical accuracy. The model was subsequently used to investigate the effect of the flooded lagoon area enlargement on tidal propagation in Ria de Aveiro. Simulations were performed for three geomorphologic configurations, representing the reference or present situation and two flooded scenarios. Results were compared through the analysis of tidal currents, tidal asymmetry and tidal prism.

The increase of the lagoon flooded area results in an intensification of the tidal currents, tidal prism and tidal asymmetry. Results also indicate that the tidal prism further increases when the flooding depth increases. Otherwise, changes in tidal currents and in tidal asymmetry pattern are negligible with the increase of the flooded area depth.

These results indicate that modifications of the flooded area of estuarine systems will result in tidal changes, with an intensification of the actual tidal patterns induced by the enlargement of inundation areas.

1. Introduction

Coastal environments occupy one of the most dynamic interfaces on Earth, at the boundary between land and open sea, and support some of the most diverse and productive habitats. Around the world, these systems experience the increased rates of changes in their geomorphology especially due to coastal erosion which is, amongst others, attributed to rising sea levels, the reduced amount of sediment delivery to the coast as well as the anthropogenic degradation (Alves et al., 2009; Santos and Miranda, 2006). These pressures together, make these coastal systems more vulnerable to risks of flooding and therefore to an increase of their flooded areas.

Besides the previously referred factors, an important aspect concerning the possible enlargement of the flooded areas lies in the lack of conservation and maintenance of the coastal systems.

Therefore, although rising global sea levels is an important factor determining the estuarine flooded areas, the local and regional-scale processes (some of them of anthropogenic origin) will also induce changes in coastal systems. Tidal propagation in this kind of environments depends strongly on their geomorphologic configuration. Changes in tidal propagation influence the sediment balance in the systems, and therefore modify their potential to export sediment and consequently their morphology. Since these changes are not fully understood, it is important to investigate how these local processes will affect the dynamic of the coastal systems.

The poor conservation and maintenance is common to a large number of coastal areas. About 75% of global salt pans are located in

---

* Corresponding author. Tel.: +351 234 370 288; fax: +351 234 378 197.
E-mail addresses: ana.picado@ua.pt (A. Picado), joao.dias@ua.pt (J.M. Dias), afortunato@lnec.pt (A.B. Fortunato).

0278-4343/$ - see front matter © 2010 Elsevier Ltd. All rights reserved.
doi:10.1016/j.csr.2010.08.012

northern and central Mediterranean countries, Spain, Greece, Italy, France and Portugal (Crisman et al., 2009), with a large number of them located inside estuarine systems. However, the production of salt is declining, as a consequence of the low profitability of the sector. Some of the salt pans completely disappeared due to the drastic change in land use (industrialization and urbanization). Other abandoned salt pans were replaced by aquaculture tanks, or have gradually degraded as a result of solid waste disposal, or simply due to the lack of maintenance. The abandonment and consequent degradation of the salt pans could contribute to the erosion, provoke bathymetric and geometric changes and could increase the flooded areas of some coastal systems.

The Ria de Aveiro (Fig. 1), a mesotidal lagoon located on the Northwestern Portuguese coast, is characterized by a large number of mostly abandoned salt pans, which are in a progressive degradation process due to the lack of maintenance and to the strong currents occurring in the nearby channels which erode their protective walls.

Inspite of the importance of evaluating tidal changes induced by geomorphologic modifications, only one previous work focusing on Ria de Aveiro tidal changes was found (Araújo et al., 2008) and only a few were found about its tidal asymmetry (Dias, 2001; Lopes et al., 2006; Oliveira et al., 2006a; Araújo et al., 2008). However the influence of local geomorphologic modifications, namely the study of flooding scenarios in this lagoon was never investigated. Moreover, the number of studies found about tidal changes induced by geomorphologic modifications at worldwide estuaries or lagoons is very scarce (e.g.: Harvey, 1988; Malhadas et al., 2009).

Araújo et al. (2008) reported an average increase of 0.245 m in M_2 amplitude and 17.4° decrease in M_2 phase in the Ria de Aveiro, over 16 years (1987–2004). They investigate the causes of these changes through a sensitivity analysis of the response of the main tidal constituent, M_2, to variations in: lagoon surface area, inlet channel depth and bottom friction. The results confirm that the changes in the bathymetry of the inlet channel are the most significant contribution to the tidal changes observed. However, they also revealed that significant changes in tidal characteristics may be expected in response to changes in the lagoon surface area.

Concerning tidal asymmetry, Dias (2001) and Lopes et al. (2006) characterized the first half of the main channels of the Ria de Aveiro lagoon as ebb dominant and the second half as flood dominant. The results from Oliveira et al. (2006a) confirm this pattern, showing differences between ebb and flood durations revealing that the system shifts from mildly ebb dominant at the mouth to strongly flood dominance in the upper reaches of the lagoon. Araújo et al. (2008) reported that during 1987/1988, the majority of the lagoon was flood-dominant, and that since then the central section of the lagoon has become ebb-dominant, whilst the northern and southern sections remain flood-dominant. All these studies show that the ratio between the amplitudes of the M_4 and the M_2, regarded as a measure of tidal asymmetry, is very small near the lagoon mouth increasing along the channels.

Harvey (1988) showed that the reduction of the flooded area associated with the construction of a dam in Murray estuary led to a significant decrease in tidal prism. Malhadas et al. (2009) investigate the effect of bathymetric changes on tidal propagation and residence time (RT) in the Óbidos Lagoon. The results revealed that tidal propagation strongly depends on bathymetric configuration and also suggest that dredging operations and the relocation of the inlet may increase the tidal prism of the lagoon leading to a reduction of the RT in its central area.

Thus, the main aim of this paper is to investigate the effect of geomorphologic changes on tidal propagation in estuarine systems, through the analysis of the Ria de Aveiro which is at risk of flooding. In this situation the changes are associated with the collapse of the salt pans walls that increase the flooded area and may affect the overall lagoon's hydrodynamics and the bottom morphology in unknown ways that must be clarified.

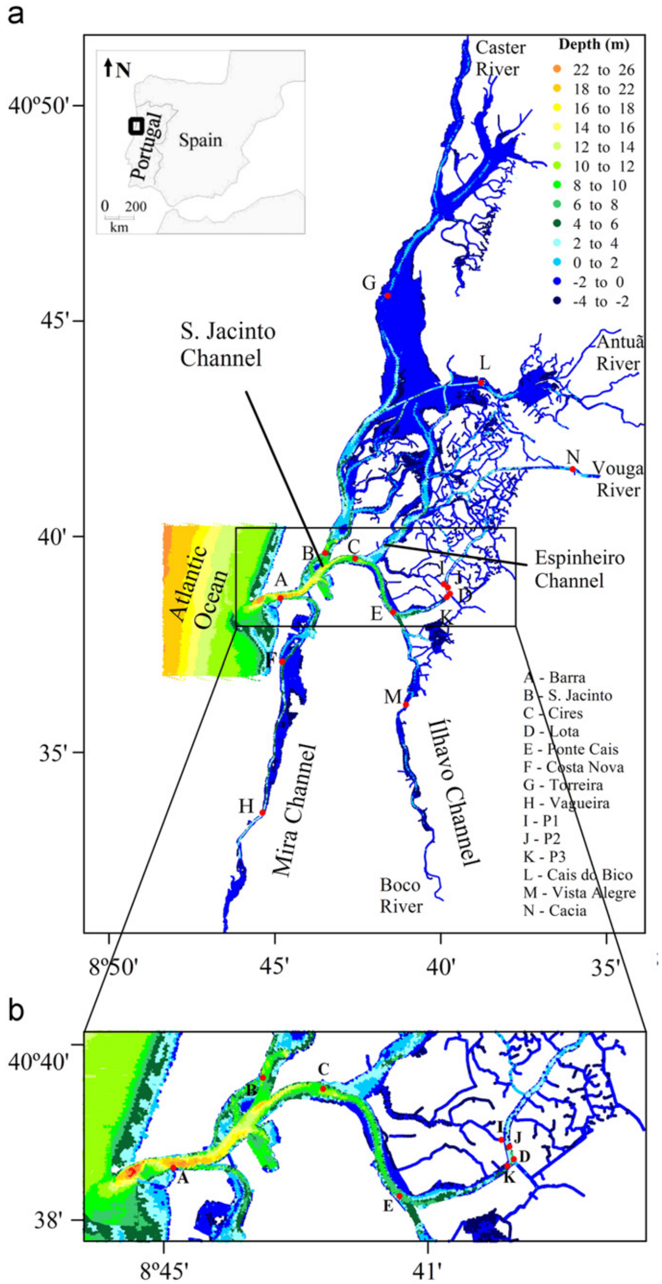

Fig. 1. Ria de Aveiro bathymetry, represented in geographic coordinates, with depth in metres relative to the local chart datum (2.0 m below the mean sea level) and with locations of the stations where field data are available. (a) Entire lagoon and (b) enlargement of the study area.

To evaluate the impact of geomorphologic changes in Ria de Aveiro, which may be generalized to other similar systems, several possible future scenarios were simulated, in which salt pans walls destruction was assumed. These simulations were performed with the shallow water numerical model ELCIRC (Zhang et al., 2004), whose implementation and calibration is also described in this study.

2. The study area

The Ria de Aveiro (40°38′N, 8°44′W) (Fig. 1) constitutes a very important coastal system in the Portuguese west coast, with an adjacent area of about 250 km^2. It is the most extensive Portuguese lagoon system and the one most dynamic in terms of physical and biogeochemical processes. The system is characterized by a large number of channels between which lie significant intertidal areas, essentially mudflats, salt marshes and old salt pans. The evolution of the Ria de Aveiro during the 20th century has been characterized by the erosion of these intertidal areas and widening of most channels. These changes, together with other anthropogenic contributions, are believed to have modified the tidal dynamics of the system, making it more vulnerable to risks of flooding and to sea level rise (da Silva and Duck, 2001).

The lagoon has a maximum width of 10 km and its length measured along the longitudinal axis is 45 km (Dias and Lopes, 2006a, b). The average depth of the lagoon relative to the mean sea level is about 3 m, although the inlet channel can exceed 28 m deep, due to dredging operations that are frequently carried out to allow the navigation. Due to the small depth and to the significant tidal amplitude there are zones, especially along the borders of the lagoon and in its central area, which are alternately wetted and dried during each tidal cycle.

The Ria de Aveiro is connected to the sea by a 350 m wide inlet, fixed by two jetties. Despite these maritime structures, important morphological changes have occurred in this area. Until recently, the Aveiro Harbour Administration has regularly dredged the sand that accumulates at the inlet due to the southward littoral drift along the West Portuguese coast. Recent bathymetric surveys reveal erosion at the entrance channel close to the north jetty, and sand deposition close to the south jetty (Plecha et al., 2007).

The tides at the mouth of the lagoon are predominantly semidiurnal (M_2 constituent dominance), with a mean tidal range of about 2.0 m. The minimum tidal range is 0.6 m (neap tides), and the maximum tidal range is about 3.2 m (spring tides), corresponding to a maximum and a minimum water level of 3.5 and 0.3 m, respectively (Dias et al., 2000).

The major fluvial input comes from the Vouga (50 m^3 s^{-1} average flow) and Antuã rivers (5 m^3 s^{-1} average flow). The Vouga River contributes with around 2/3 of the freshwater entering the lagoon (Moreira et al., 1993; Dias et al., 1999). However, river flows into the lagoon were neglected, because the total mean fresh water discharge into the lagoon during a tidal cycle is about 1.8×10^6 m^3 (Moreira et al., 1993) while the tidal prism is 137×10^6 m^3 for maximum spring tide and 35×10^6 m^3 for minimum neap tide (Dias et al., 2000). The Ria de Aveiro is vertically homogeneous during dry seasons, but stratification becomes important near the freshwater inflow locations after important rainfall (Dias et al., 1999; Vaz and Dias, 2008). A small artificial headland (Triângulo Divisor das Correntes) divides the entrance channel in two different arms, separating the tidal prism of an incoming tide in two flows: a small one flowing into the Mira channel and a second more important one flowing to the S. Jacinto, Espinheiro and Ílhavo channels. The tidal prism in each of the main channels relative to its value at mouth is about 35% for the S. Jacinto channel, 26% for the Espinheiro channel, 10% for the Mira channel and 14% for the Ílhavo channel (Dias et al., 2000).

The salt pans of Aveiro occupies about 15 km^2, but many of them are now abandoned or replaced by aquaculture tanks, as a consequence of the low profitability of the sector. Due to the lack of maintenance of the abandoned salt pans, their protective walls are destroyed by the strong currents inside the lagoon as well as by the vessels' wake waves. As this destruction will result in a significant increase of the flooded area in Ria de Aveiro, it may affect the overall lagoon's hydrodynamics and the bottom morphology in unknown ways. The number of active salt pans steadily decreased from 500 in the 15th century to 270 fifty years ago, and only eight remaining presently. The salt pans currently occupy the marsh areas and only a few are accessible by land.

Fig. 2. The salt field of Aveiro lagoon obtained in 2007 by Digital Globe.

The salt field of Aveiro is divided into five groups: S. Roque, Sul, Mar, Norte and Monte Farinha (Fig. 2). Due to its large extension, it was impossible to perform a comprehensive study of all salt pans. Therefore, this work focuses on the Mar group and the southern part of the Norte group that are the most vulnerable to strong currents.

3. Methodology

A previous ELCIRC model implementation to Ria de Aveiro (Oliveira et al., 2006a) was refined and then applied in this investigation. Due to the low resolution of the horizontal grid developed by those authors for the narrow channels around the salt pans, the grid was considerably improved in this study, adding and refining several channels, mainly in the central area of the lagoon, where salt pans are located (Fig. 3).

The present analysis combines recent field data with numerical models. First, water level data were used to calibrate the hydrodynamic model. Afterwards the bathymetry configuration scenarios were established and used in the detailed, numerically based hydrodynamic analysis.

The model calibration was performed at 14 stations (A–N) within the lagoon (Fig. 1), with a depth-dependent Manning coefficient (Table 1), whose values were based on the ones presented by Dias and Lopes (2006a, b). The Manning values were locally adjusted until the model outputs reproduce accurately the field data.

In order to evaluate the influence of the new bathymetry in the model's ability to reproduce the Aveiro lagoon hydrodynamics as well as the model's accuracy, comparisons between the model results obtained in this work, those obtained by Oliveira et al. (2006a) and the field data were performed.

Afterwards, the hydrodynamic model was used to characterize the response of the lagoon hydrodynamics to the increase of the flooded area and volume, due to the salt pans walls collapse. Therefore, a new grid was generated representing the flooding of the Ria de Aveiro central area (Fig. 4). The inundation was achieved through the partial collapse of the degraded salt pans walls, whose dimensions are in accordance with the ones presented in INTERREG III B (2008) and with satellite images. For lack of information on the depth of the salt pans, a sensitivity analysis to this depth was performed. This depth was set to 1 and 3 m below to the mean sea level (i.e., −1 and 1 m relative to the local chart datum). To evaluate the impact of the changes in the

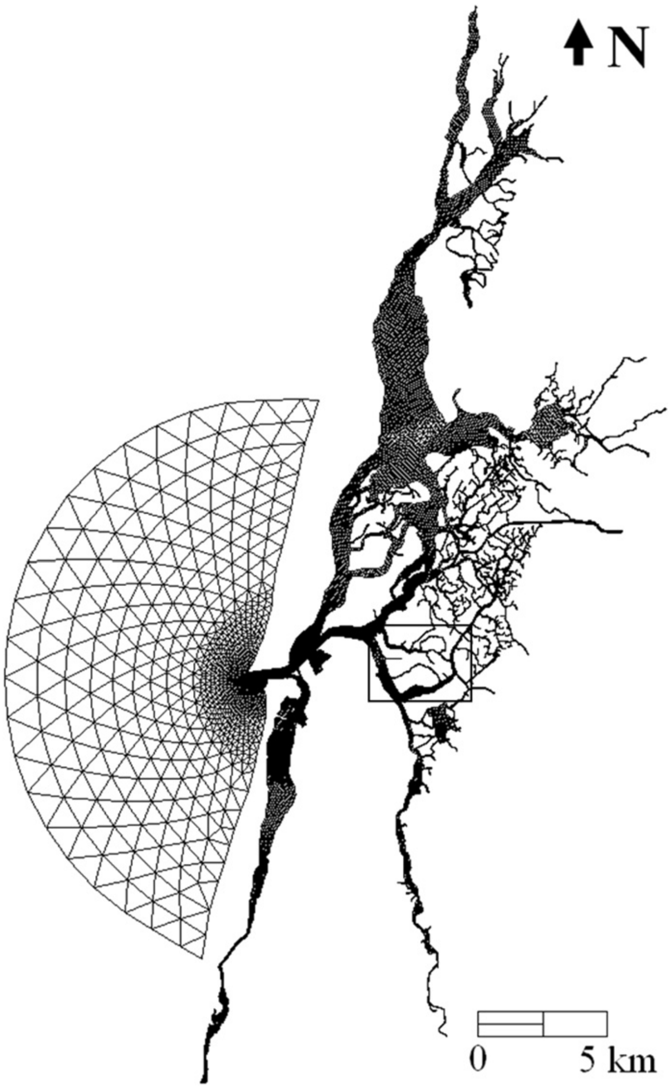

Fig. 3. Horizontal grid of the Ria de Aveiro, with 71 996 nodes and 94 352 elements.

Table 1
Bottom friction coefficients.

Depth (m)	Manning's *n* values
$-1 \leq h < -0.5$	0.026
$-0.5 \leq h < 0.0$	0.024
$0.0 \leq h < 0.5$	0.022
$0.5 \leq h < 1.0$	0.020
$1.0 \leq h < 3.0$	0.018
$3.0 \leq h < 6.0$	0.016
$6.0 \leq h < 10.0$	0.015
$h \geq 10.0$	0.014

total area and volume in a system like Ria de Aveiro, the model ELCIRC was run for the present bathymetry and for both case studies. The evaluation was performed through the analysis of tidal currents, tidal prism and tidal asymmetry.

3.1. Field data

Data available for this study are from two distinct field campaigns, from 2003 and 2006. Sea surface elevations were collected hourly, during a tidal cycle, very close to the salt pans area under analysis, in the framework of SAL project—Sal do Atlântico (UE—INTERREG III B Espaço Atlântico, 2004–2007), at stations I, J and K (Fig. 1). Sea surface elevations at the other eleven stations were measured during a month every 6 min, except at Torreira, where measurements were performed every half-hour. These data were collected in the framework of the Ph.D. Thesis of Araújo (2005).

The bathymetric data (Fig. 1) available for this study were collected in a general survey carried out in 1987/1988 by the Hydrographic Institute of Portuguese Navy (IH). Because dredging operations were performed in 1998 in the Mira and the S. Jacinto channels, and due to the morphological changes at the inlet channel previously reported data from recent surveys performed by the Aveiro Harbour Administration close to these areas were used to update the bathymetric database in these regions.

3.2. Hydrodynamic model

3.2.1. Model description and setup

ELCIRC (version 5.01.02g) is a model designed for the effective simulation of three-dimensional baroclinic circulation across river-to-ocean scales. The model ELCIRC uses a finite-volume/finite difference Eulerian–Lagrangian algorithm to solve the shallow water equations, written to realistically address a wide range of physical processes and of atmospheric, ocean and river forcings (Zhang et al., 2004).

Although ELCIRC is a fully 3D baroclinic model, it was used herein in barotropic mode and with a single vertical layer. Due to the shallow depths and minor freshwater inputs to the Ria de Aveiro, its circulation can adequately be simulated with a depth-averaged model.

The depth-integrated equations solved in this model express the conservation of mass and momentum:

$$\frac{\partial \eta}{\partial t} + \frac{\partial [HU]}{\partial x} + \frac{\partial [HV]}{\partial y} = 0 \tag{1}$$

$$\frac{\partial U}{\partial t} + U\frac{\partial U}{\partial x} + V\frac{\partial U}{\partial y} = fV - g\frac{\partial \eta}{\partial x} - \frac{\tau_x}{\rho} + \varepsilon\left(\frac{\partial^2 U}{\partial x^2} + \frac{\partial^2 U}{\partial y^2}\right) \tag{2}$$

$$\frac{\partial V}{\partial t} + U\frac{\partial V}{\partial x} + V\frac{\partial V}{\partial y} = -fU - g\frac{\partial \eta}{\partial y} - \frac{\tau_y}{\rho} + \varepsilon\left(\frac{\partial^2 V}{\partial x^2} + \frac{\partial^2 V}{\partial y^2}\right) \tag{3}$$

where $H(x,y)=h(x,y)+\eta(x,y,t)$ is the total water depth, $\eta(x,y,t)$ is the surface water elevation, $h(x,y)$ is the water depth, g is the acceleration of gravity, t is the time, U and V are the depth-averaged velocity components in the x (eastward) and y (northward) directions, ρ is the water density, ε is the horizontal eddy viscosity, τ_x and τ_y are the bottom stress according to each horizontal direction and are defined in the following form:

$$\tau_x = \rho C_D \sqrt{U^2 + V^2}\,U \tag{4}$$

$$\tau_y = \rho C_D \sqrt{U^2 + V^2}\,V \tag{5}$$

where C_D is the drag coefficient and ρ is the reference density. Wind stress was not considered. The drag coefficient is computed with a Manning law, i.e.:

$$C_D = gn^2 H^{-1/3} \tag{6}$$

where n is a space-dependent Manning coefficient. Eddy viscosity is neglected, as the horizontal grid resolution is considered sufficient to resolve the relevant scales.

The numerical algorithm of ELCIRC used a semi-implicit scheme. The barotropic pressure gradient in the momentum equation and the flux term in the continuity are treated semi-implicitly, with implicitness factor $0.5 \leq \theta \leq 1$. According to

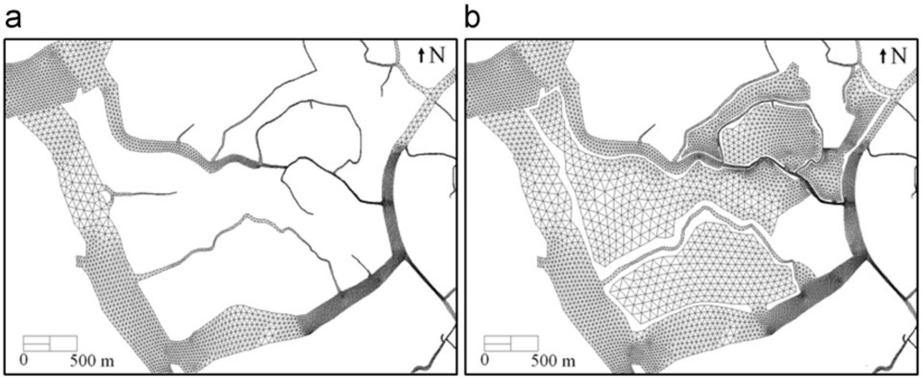

Fig. 4. Detail of the horizontal grid near the study area: (a) present configuration and (b) configuration resulting from the salt pans walls destruction.

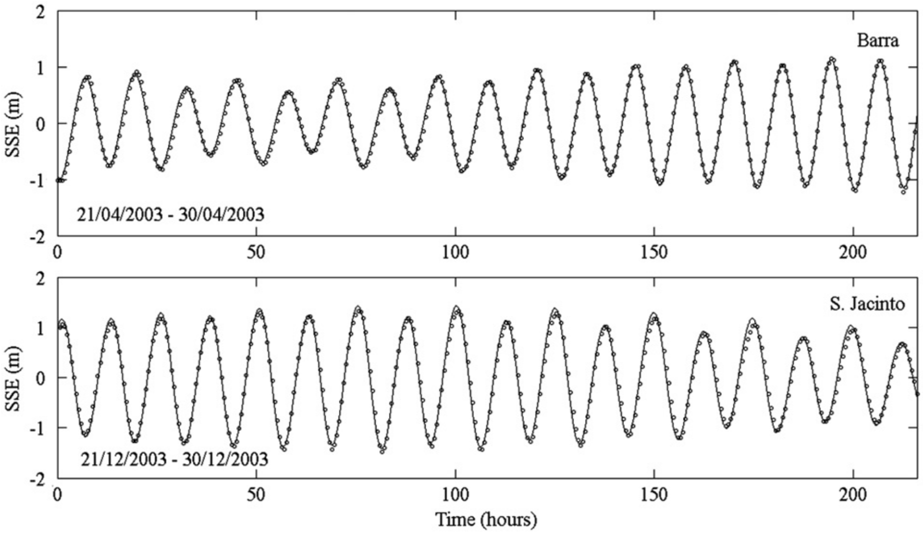

Fig. 5. Comparison between predicted and observed SSE (solid line: model results; circles: measurements). In the panels are referred the beginning and the end of each compared period.

Casulli and Cattani (1994) this ensures both stability and computational efficiency.

Flexibility in discretizing complex bathymetries and geometries, like in the Ria de Aveiro, is achieved through unstructured grids in the horizontal plane.

The Ria de Aveiro was discretized with a horizontal grid with an area of about 210 km^2, 94 352 triangular elements and 71 996 nodes.

The hydrodynamic model was forced by fourteen harmonic constituents (Z_0, M_{SF}, O_1, K_1, P_1, Q_1, N_2, M_2, S_2, K_2, M_4, MN_4, MS_4 and M_6) taken from the regional model of Fortunato et al. (2002a), and freshwater input was neglected. The time step was set to 90 s to prevent the appearance of oscillations due to wetting and drying.

3.2.2. Hydrodynamic model calibration

The hydrodynamic model calibration was performed at 14 stations within the lagoon, with a depth-dependent Manning coefficient (Table 1). The Manning values were based on the ones presented by Dias and Lopes (2006a, b) and were locally adjusted until the model outputs agreed satisfactorily with the field data. Since Ria de Aveiro has a very complex geometry, with depths varying between −2 m in the intertidal zones and approximately 30 m in the navigation channel, is deemed important that the Manning values were adjusted to the local characteristics and therefore vary with depth.

The hydrodynamic model was forced in the oceanic boundary by tides only, so in order to compare model results with measurements, the low frequency signal was removed from the data, using a cut-off frequency of 0.0000093 Hz (30 h). For consistency, the same filter was applied to the model results.

Table 2
RMSE, percentage of RMS errors relative to the local amplitude and predictive skill for all the calibration stations.

Station	RMSE (m)	Δ (%)	Skill
A	0.1087	9.89	0.9815
B	0.0865	8.69	0.9919
C	0.1674	15.25	0.9864
D	0.2298	23.05	0.9785
E	0.1486	10.02	0.9768
F	0.0837	8.58	0.9931
G	0.2301	28.57	0.8244
H	0.3148	35.60	0.7909
I	0.1443	9.62	0.9661
J	0.2476	16.51	0.8042
K	0.1927	9.98	0.9468
L	0.3201	38.68	0.7340
M	0.3574	42.39	0.9070
N	0.2299	26.92	0.9761

The methodology used herein, and based on several studies (Dias et al., 2009; Oliveira et al., 2006b), for models calibration in estuarine systems dominated by tides is performed mainly in the high-frequency domain, once it is the dominant signal intended that the models reproduce with great accuracy. Moreover, the Ria de Aveiro is mainly forced by tides, being the atmospheric local effects important only during short periods and in reduced areas (Dias et al., 1999; Dias and Fernandes, 2006). The non-local atmospheric effects induce the meteorological tide that consists in an additional elevation to the astronomical tide that can be considered at the ocean boundary condition, and therefore is well reproduced by the model.

Initially, the calibration was performed by comparing model results with observed sea surface elevation (SSE) (see comparison for 2 of the stations in Fig. 5). The visual comparison between the predicted and observed SSE reveals model's ability to reproduce the data.

The calibration was assessed for skill through the determination of the root mean square errors (RMSE) and the predictive skill at each station, as well as through the comparison of the harmonic constants determined from the model and the data at 11 stations.

According to Dias et al. (2009), the RMS errors should be compared with the local tidal amplitude. If they are lower than 5% of the local amplitude, the agreement between model results and observations should be considered excellent. If they range between 5% and 10% of the local amplitude the agreement should be considered very good.

The model predictive skill is based on the quantitative agreement between model results and observations (Warner et al., 2005). Perfect agreement between model results and observations would yield a skill of one and complete disagreement would yield a skill of zero. Skill values higher than 0.95 indicate an excellent agreement between model results and observations (Dias et al., 2009).

The RMS errors and the skill were computed for each station and are summarized in Table 2. RMSE values range from 8% to 10% of the local amplitude for the stations A, B, E, F, I and K, and therefore the predictions are considered very good. However, RMS errors exceed 10% of the local amplitude at the other stations.

An RMS error of about 10 cm was found for the station located at the lagoon mouth (station A), i.e., around 5% of the local mean tidal range. The best model results were obtained for the stations closest to the lagoon's mouth (e.g. station B with a RMSE of about 9 cm) and the highest disagreements were found for stations G, H, L and M with RMS errors around 15% of tidal range and with skill values lower than 0.95.

The errors found may be partially attributed to small inaccuracies on the tidal forcing on the ocean open boundary, to the deficient representation of the very narrow channels in the horizontal grid, to possible inaccuracies in the bathymetry as well as to possible uncertainties in the field data.

The RMSE and skill results are similar to those obtained for other coastal systems in Portugal, based on the use of ELCIRC and other hydrodynamic models (Oliveira et al., 2006b, c; Fortunato et al., 1999, 2002b; Dias and Lopes, 2006a, b; Dias et al., 2009).

There is a large disadvantage on the direct comparison of RMSE and skill errors, since phase and amplitude errors are considered together. In addition, tidal asymmetry, which will be analysed below, is mostly determined by the relative importance of the major constituent (M_2) and its first higher harmonic (M_4). Thus, harmonic analysis was done for both predicted and observed SSE in order to quantify separately the amplitude and phase differences for all stations, with exception of I, J and K stations because the available data for these stations only have the duration of 11 h. This procedure was performed using the t_tide matlab® package of Pawlowicz et al. (2002).

Distributions of tidal amplitudes and phases for the major tidal constituents (M_2, S_2, O_1, K_1 and M_4) in the Ria de Aveiro are presented in Fig. 6.

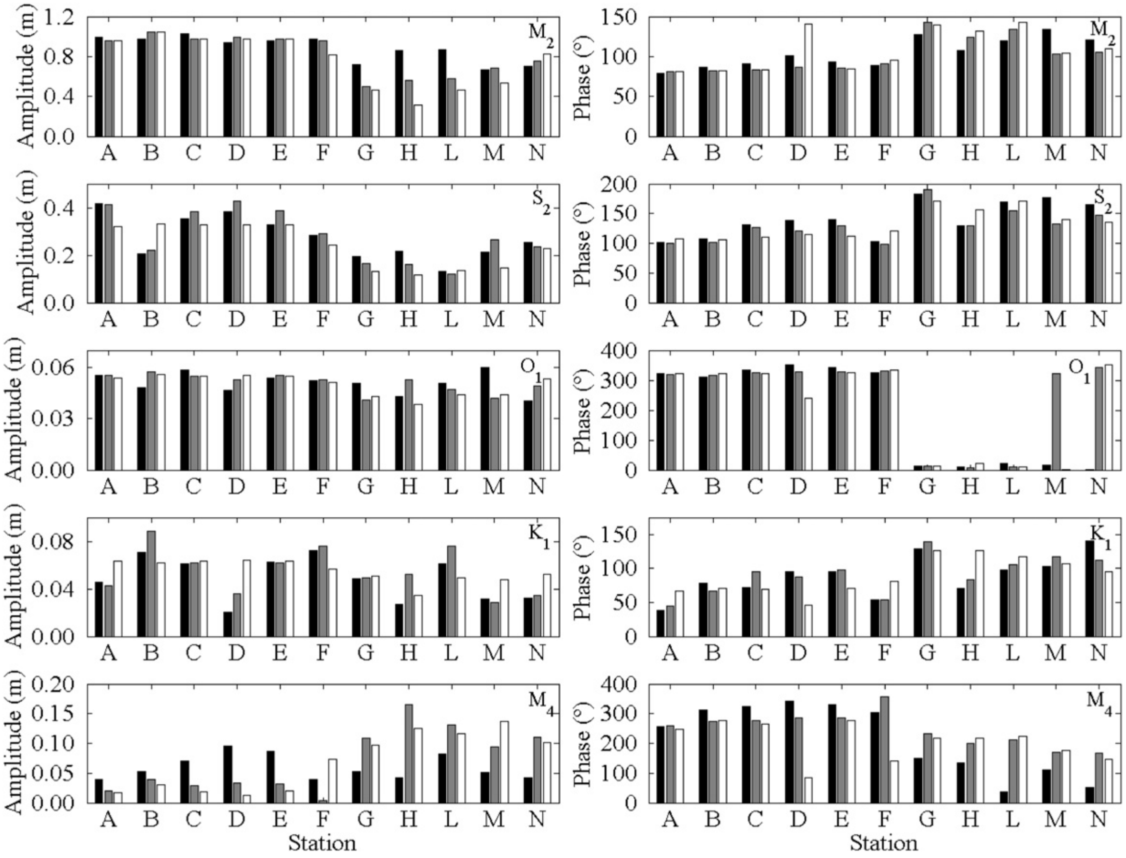

Fig. 6. Distributions of tidal amplitude and phase for M_2, S_2, O_1, K_1 and M_4 constituents (black: measurements; gray: model results and white: Oliveira et al., 2006a) results.

The agreement between predicted and observed values is good both in amplitude and in phase for the semidiurnal constituents, which are the major tidal constituents in Ria de Aveiro. For the major constituent (M_2), the mean difference between predicted and observed amplitudes is about 10 cm. This value was amplified by the errors found for stations G, H and L that present a mean difference of about 16 cm. If the values for these stations are not considered, the mean difference between predicted and observed amplitudes is about 4 cm.

For the S_2 constituent, the mean difference between predicted and observed amplitude is about 3 cm. In fact, the model results represent the amplitude of the S_2, at the stations G, H and L, more accurately than the amplitude of M_2, which reduces the S_2 amplitude mean difference.

The mean phase difference for both semidiurnal constituents is about 12°, which means that the average delay between the predicted and observed tide is about 24 min. This delay is larger than was expected, mainly due to the phase difference at stations L and M. At station L the phase difference is approximately 14° (29 min) for both semidiurnal constituents and at station M the phase difference is approximately 40° (60 min) for the M_2 constituent and 40° (80 min) for S_2.

The results for the diurnal constituents (O_1 and K_1) can also be considered good at all stations, but reveal a worse agreement between model predictions and data. For instance, it was found an amplitude error of about 25% at station G and about 43% at station M for O_1 constituent. For K_1 constituent the major amplitude error was around 45% at stations D and H.

The M_4 constituent was not simulated with the expected accuracy (Fig. 6). The errors found in the M_4 reproduction may be due to bathymetric errors that cannot be corrected by the adjustment of the friction coefficient. The relatively large errors associated with M_4 are not surprising, as overtides are typically much more difficult to reproduce correctly than the major astronomic constituents. In this particular case, the correct reproduction of overtides is further hampered by the changes in bathymetry over the years, which significantly affect tidal propagation. For M_2, an average increase of 0.245 m in amplitude and an average decrease of 17.4° in phase were observed over 16 years (Araújo et al., 2008). Since there is a discrepancy of about 16 years between the bathymetric and the tidal data used herein, similar discrepancies should be expected between the tidal data and the model results. While these discrepancies are partially mitigated by the calibration for the major constituents, non-linear constituents are affected by friction differently, and therefore do not match the data as well. Still, as the M_4 constituent is generated through the advective and finite amplitude terms, which are correctly represented by the model, the results for M_4 constituent are expected to be realistic enough to reproduce tidal asymmetry.

In order to evaluate the influence of the new bathymetry developed in the frame of this study in the model's accuracy in reproducing the Ria de Aveiro hydrodynamics, some comparisons between the model results obtained in this work and those obtained by Oliveira et al. (2006a) were performed. Thus, the amplitude and phase of the M_2, S_2, K_1, O_1 and M_4 constituents were compared at several stations within the lagoon (Fig. 6). Generally, the new bathymetry reproduces the lagoon hydrodynamics better than the bathymetry used by Oliveira et al. (2006a) in the central area of the lagoon. Otherwise, in the upper stations, for instance, for the M_4 constituent the results obtained by Oliveira et al. (2006a) are more accurate. Therefore, the results suggest that the limitations in the bathymetry may affect the model's accuracy in reproducing the lagoon hydrodynamics.

Table 3
Total area and volume for each bathymetry and differences relative to the present bathymetry.

Grids	**Flooded depth (m)**	**Area ($m^2 \times 10^6$)**	**Volume ($m^3 \times 10^6$)**	Relative to the present bathymetry	
				ΔArea (%)	**ΔVolume (%)**
Present bathymetry		55.66	98.04	–	–
Flooded case	1	58.78	101.46	5.61	3.49
	3		107.30		9.45

4. Results and discussion

4.1. Model-based hydrodynamic analysis

Model results were compared for simulations conducted for three geomorphologic configurations, which represent the system under different conditions: present bathymetry and bathymetries representing the salt pans walls collapse, as represented in Fig. 4. Two tests were performed regarding to the flooded depth: the depth was set to 1 and 3 m below the mean sea level, in order to study the lagoon hydrodynamics sensitivity to changes in the volume of the flooded area. The total area and volume of the entire lagoon below the mean sea level for the bathymetries studied are quantified in Table 3.

Possible changes in the lagoon hydrodynamic regime, due to geomorphologic changes, are evaluated in the next sections. This evaluation is performed through the analysis of the tidal currents, the tidal asymmetry along the axis of the main channels of the lagoon and the tidal prism for several cross-sections along the lagoon, determined for each simulation.

4.1.1. Tidal currents

In this section, the response of the magnitude of flood and ebb velocities to geomorphologic changes in the lagoon central area is evaluated.

The velocities are represented near the lagoon mouth on maximum flood and ebb at spring tides, for the present bathymetry and for the two flooded depth tests projected (Fig. 7). In Fig. 8 the differences between the velocity of the two depth tests and the present bathymetry are represented for the same period represented in Fig. 7. Thus, the positive values indicate that the velocity of the depth tests is greater than the velocity of the present bathymetry. Conversely, negative values indicate a lower magnitude of velocity for the depth tests.

Generally, for all the configurations the model results show that velocities are systematically stronger on ebb than on flood, revealing ebb-dominance of the central area of the lagoon.

Model results indicate that the tidal velocities increase from the present configuration to the flooded cases. According to the model results, at spring tides, maximum ebb and flood velocities are 1.94 and 1.85 ms^{-1}, respectively, for the present configuration, and 2.06 and 1.96 ms^{-1} for both tests projected, which corresponds to increases of about 5–6% (Table 4). At neap tides, near the lagoon inlet, the growth of the maximum velocities increases to about 6–14% for both tests. The largest differences of the magnitude of velocity are observed along the navigation channel and during the ebb (Fig. 8). In the north area adjacent to the south breakwater, the differences are negligible, because this is a sheltered area with low velocities.

Velocities were also analysed for the entire lagoon, showing that the increase of the tidal currents with the expansion of the flooded area is enhanced near the flooded location. In conclusion,

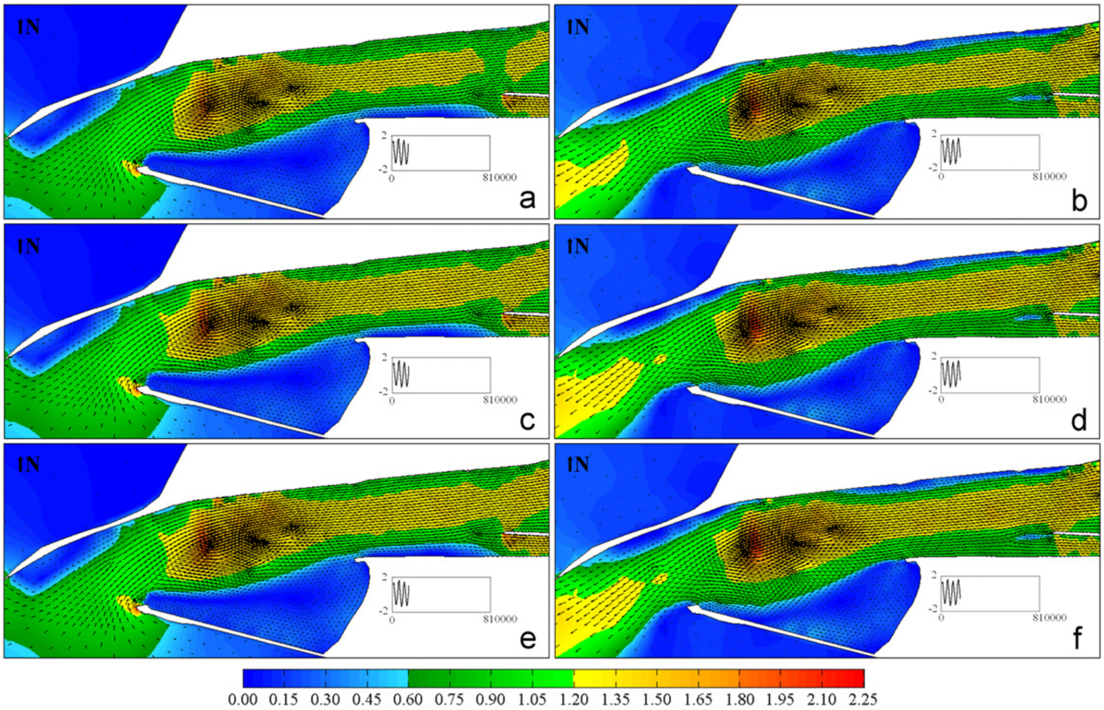

Fig. 7. Magnitude of velocity in ms^{-1} during the spring tide near the inlet of the lagoon. Left: flood and Right: ebb currents for the present bathymetry (a and b), configuration with the flooded depth set to 1 m (c and d) and configuration with the flooded depth set to 3 m (e and f).

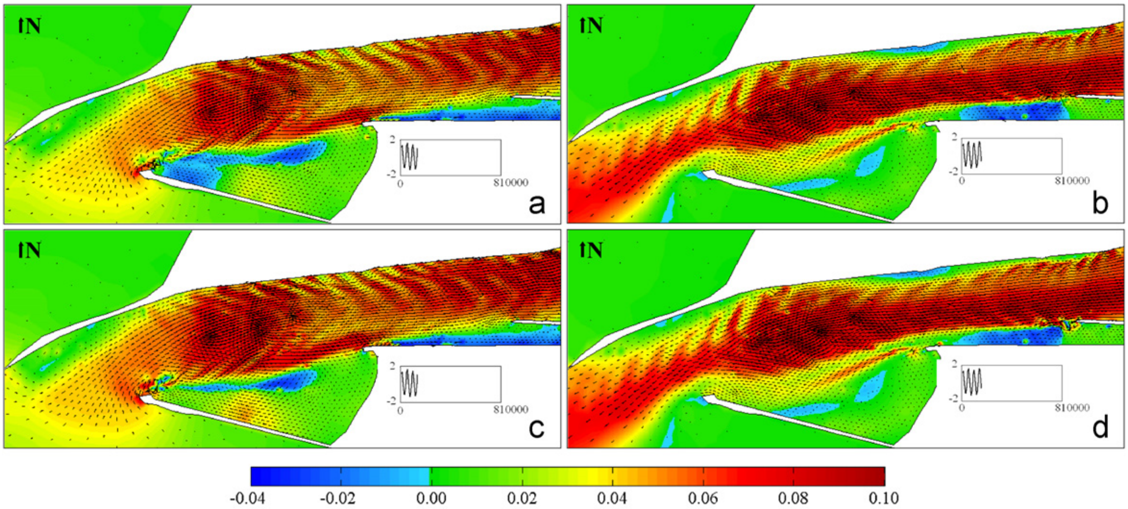

Fig. 8. Velocity differences between the configuration with the flooded depth set to 1 m and present bathymetry (a and b) and between configuration with the flooded depth set to 3 m and present bathymetry (c and d). Left: flood and right: ebb currents.

changes in the lagoon area induce higher velocities near the inlet, with the more significant increase on neap tides and near the flooded area. Model results also indicate that increasing the flooded depth from 1 to 3 m has little influence on the magnitude of velocities in the lagoon. In fact, the surface area of the lagoon relative to the cross sectional area of the channels does not change much and therefore great changes in the velocity fields are not expected.

4.1.2. Tidal asymmetry

Along much of the world's coastlines as well as in the Ria de Aveiro, the dominant astronomical constituent is M_2, the semidiurnal lunar tide. Because of M_2 dominance, the most significant overtide formed in these well mixed estuaries is M_4, the first harmonic of M_2 (Friedrichs and Aubrey, 1988), which is generated primarily through the advective and finite amplitude terms. In the Ria de Aveiro, the amplitude of the M_4 constituent increases from the lagoon mouth upstream. The most important consequence of this growth is the differentiation of the ebb and flood durations, which is an indicator of an asymmetric tide.

A direct measurement of non-linear distortion, the M_4 to M_2 sea-surface amplitude ratio indicates the magnitude of the tidal asymmetry generated within the estuary. An undistorted tide has an amplitude ratio of zero. The larger the amplitude ratio, the more distorted the tide is, and the more strongly flood or ebb

Table 4
Magnitude of the maximum velocity in ms^{-1} near the inlet and differences relative to the present bathymetry at spring and neap tides.

	Flooded depth (m)	Magnitude of velocity (m/s)							
		Neap tide				Spring tide			
		Max. flood	Δ (%)	Max. ebb	Δ (%)	Max. flood	Δ (%)	Max. ebb	Δ (%)
Present bathymetry		0.43	–	0.60	–	1.85	–	1.94	–
Flooded case	1	0.47	9.30	0.64	6.67	1.96	5.95	2.06	6.19
	3	0.49	13.95	0.65	8.33	1.96	5.95	2.06	6.19

dominant the system becomes. The sea-surface phase of M_4 relative to M_2 is defined as $\varphi = 2\theta_{M_2} - \theta_{M_4}$ and it determines the type of tidal distortion ($0^\circ < \varphi < 180^\circ$ indicates flood dominance and $180^\circ < \varphi < 360^\circ$ indicates ebb dominance).

The amplitude and the phase of M_2 and M_4 tidal constituents were analysed for the Ria de Aveiro using model results, for the present bathymetry and for the one resulting from the salt pans walls destruction (including both depth tests).

According to the model results, an increase of the lagoon total area and volume leads to a decrease in the amplitude and an increase in the phase of the major tidal constituent, M_2, along the Ria de Aveiro, in agreement with the sensibility analysis results performed by Araújo et al. (2008). For the M_4 constituent both amplitude and phase increase.

The amplitude ratio, the relative phase and the difference between ebb and flood durations were computed along the axis of the four main channels of the Ria de Aveiro. In Fig. 9, these parameters are represented for the Espinheiro and the Íllhavo channels, in order to evaluate the tidal asymmetry, as well as the response of these parameters to an increase in the lagoon total area and volume. For the Mira and the S. Jacinto channels, the changes in these parameters are negligible (not shown). Because tidal levels exhibit very small variations across the channels, all these parameters were represented along the channels axis.

The amplitude ratio is very low close to mouth growing toward the upper reaches of the lagoon and the relative phase shows that the system shifts from ebb dominant at the mouth to flood dominant in the channels head. These results confirm the patterns found by Dias (2001), Lopes et al. (2006) and Oliveira et al. (2006a).

For the ebb-flood differences, the negative values indicate ebb duration lower than the flood one (ebb currents are higher than flood currents), which leads to ebb dominance. Conversely, positive values indicate flood dominance.

The relative phase of M_4 with respect to M_2 in the Espinheiro channel decreases with the expansion of the lagoon area and volume, indicating that the characteristics of the tidal asymmetry are changing along this channel. In fact, the increase of the lagoon area results in the decrease of the ebb-flood differences along the Espinheiro channel, which means that this channel becomes more ebb dominated (Fig. 9).

At the beginning of the Íllhavo channel (~6 km away from the lagoon mouth), ebb-flood differences decrease by about 12% with the 5.6% expansion of the lagoon area.

Furthermore, if the amplitude and phase of the major tidal constituent and its first harmonic change with the increase of the lagoon area, tidal asymmetry should also be affected.

Otherwise, differences between the tidal asymmetry parameters are negligible in these two channels when the flooded depth is increased from 1 to 3 m, indicating that the flooded depth has little influence in the tidal asymmetry pattern.

The results of ebb and flood currents obtained in the previous section corroborate the increase of the ebb dominance in the lagoon central area along the time, as was referred by Araújo et al. (2008). The enhancement of ebb dominance with the increase in the intertidal area is consistent with theoretical (Friedrichs and Aubrey, 1988; Fortunato and Oliveira, 2005) and numerical (Fortunato et al., 1999) evidence.

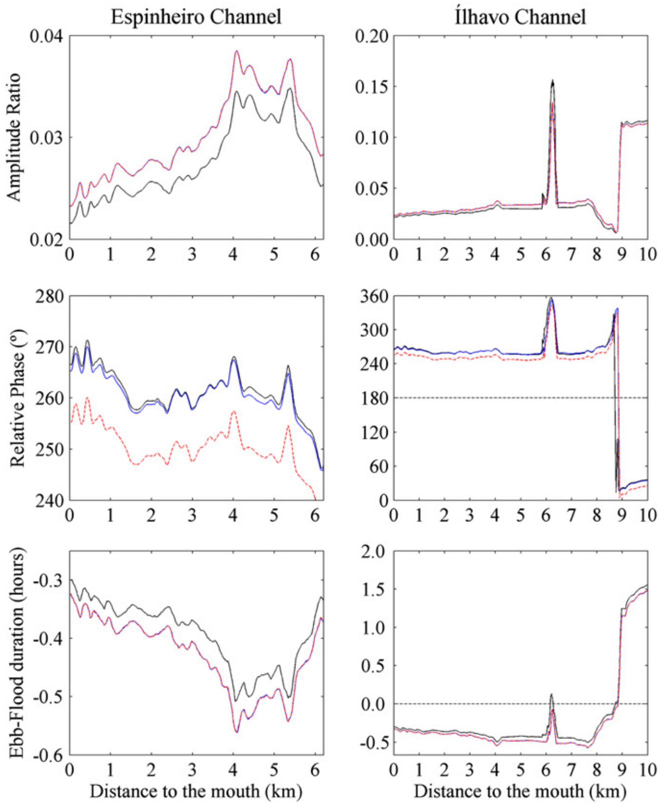

Fig. 9. Asymmetric coefficients: amplitude ratio, relative phase (deg.) and difference between ebb and flood duration (h) along the axis of the four main channels of the Ria de Aveiro. Solid line: present configuration; dashdot line: flooded depth set to 1 m and dashed line: flooded depth set to 3 m.

In summary, tidal propagation inside the lagoon depends strongly on the geomorphologic configuration. Changes in the geometry of the lagoon alter tidal propagation influencing net gain or loss of sediment to the system. In this situation, an increase in the total lagoon area results in an increase of the tidal currents, mainly on ebb, and modifies the tidal asymmetry pattern, leading to an increase of the ebb dominance, increasing the potential to export sediment.

4.1.3. *Tidal prism*

To further investigate the spatial distribution of tidal propagation and the relative importance of each channel, tidal prisms

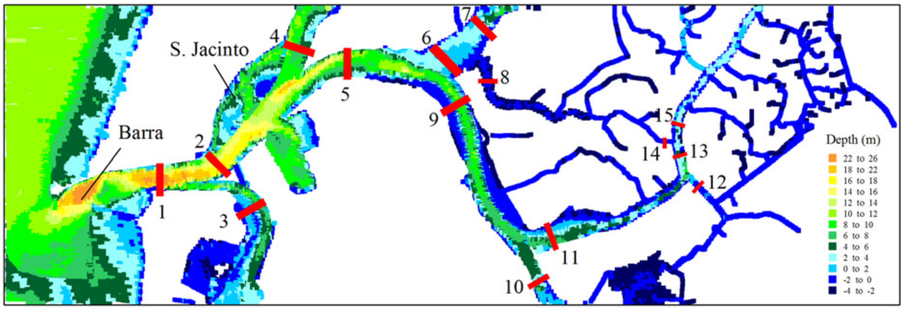

Fig. 10. Cross-section locations where the tidal prisms were computed.

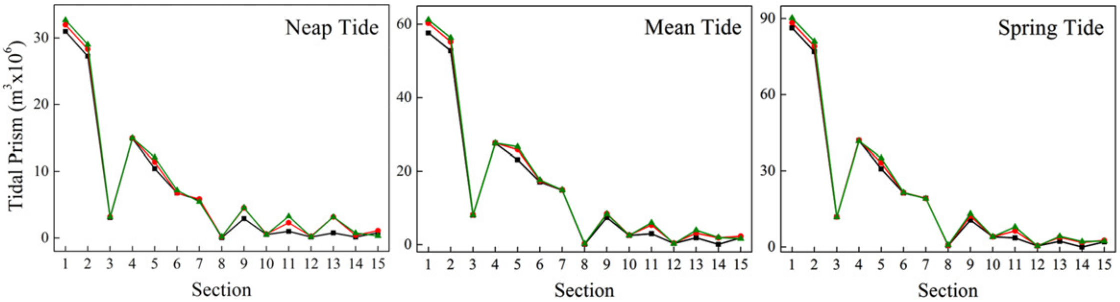

Fig. 11. Computed tidal prism at 15 cross-sections of the Ria de Aveiro during neap, mean and spring tides. Square: present configuration; circle: configuration with the flooded depth set to 1 m and triangle: configuration with the flooded depth set to 3 m.

were computed at 15 cross-sections (Fig. 10) for the present configuration and for the configurations resulting from the salt pans walls collapse, including both depth tests.

The tidal prism is evaluated herein as the volumetric flux passing through a cross-section in a flooding cycle. Clearly, the tidal prism depends not only on the location of the cross-section, but also on the tidal range. Simulations were performed for extreme spring and neap tides (~3 and ~0.7 m of tidal range at the lagoon mouth, respectively) as well as for an average tide (~1.2 m of tidal range) and the results are depicted in Fig. 11.

The relative reduction of tidal prisms from the inlet to the upper reaches of the lagoon follows a similar pattern for all the bathymetries studied. This pattern is in accordance with results obtained for other coastal systems, as for instance for the Óbidos lagoon (Oliveira et al., 2006b).

Results show that the magnitude of the tidal prisms also depends heavily on the geomorphologic configuration. The increase of the lagoon area, resulting from the large number of salt pans with their walls destroyed, enhances the tidal prism in the Ria de Aveiro. According to the model results, an increase of 5.6% in the lagoon total area leads to an increase of 2% for the maximum spring tide, for the tidal prism at the inlet. The tidal prism increases by about 5% for an average tide and by 3% for the neap tide condition.

The highest relative increase in the tidal prism was found near the flooded area, which is induced by the large increase of the lagoon area near cross-section 14, due to the salt pans walls collapse around that channel.

Contrary to the tidal asymmetry and tidal currents results, there are differences when the flooded depth is increased from 1 to 3 m. In fact, an increase of about 2% for the maximum spring tide in the tidal prism was observed at the inlet.

Since tidal prisms are common indicators of the water renewal capacity, results suggest that an increase in the lagoon total area and volume reduces residence times in the lagoon central area, which leads to a better water renewal and mitigates the water pollution effects.

These results agree with previous studies for other coastal systems. Harvey (1988) showed that the decrease of the flooded area in Murray estuary induced an important reduction in its tidal prism. Malhadas et al. (2009) reported that tidal propagation strongly depends on bathymetric configuration of Óbidos lagoon and that dredging operations and the relocation of its inlet will enlarge the lagoon tidal prism and will decrease the RT in its central area.

5. Conclusions

The main goal of this study was to contribute to the understanding of tidal changes in estuarine systems induced by geomorphologic changes, analysing the consequences of the partial salt pan walls destruction on the entire Ria de Aveiro hydrodynamic system. With this purpose, a finite volume shallow water model (ELCIRC) was implemented and calibrated for the Ria de Aveiro.

According to the final results, the model was successfully calibrated for a very complex system as Ria de Aveiro. Indeed, the RMSE values ranging from 8% to 10% of the local amplitude and skill values higher than 0.95 were found for most stations located in the lagoon central area. Larger errors exist for the rest of stations. These errors are due to several factors, such as very narrow lagoon channels that are not well resolved by the horizontal model grid, and some possible uncertainties in the field data, as well as due to possible inaccuracies in the bathymetry. The fact that there is a 16-year time span between the measurement of the bathymetry and most tidal data should also explain part of the discrepancies. In spite of these differences, the new bathymetry reproduces better the lagoon hydrodynamics in the central area than the bathymetry developed by Oliveira et al. (2006a) in a previous ELCIRC application to Ria de Aveiro. These results suggest that limitations in the bathymetry and grid resolution may affect the model's accuracy in reproducing the lagoon hydrodynamics.

Once calibrated, ELCIRC was used to characterize the Ria de Aveiro hydrodynamics under different scenarios: present configuration and configurations resulting from the salt pan walls destruction and consequent increase of the flooding area.

In order to study the hydrodynamic responses of the Ria de Aveiro to the increase of the lagoon area as well as the increase of the flooded area depth, tidal currents, tidal asymmetry and tidal prism were analysed for each configuration.

Model results show a deformation of the tide as it propagates along the lagoon, with a growth of the quarter-diurnal constituents. This growth translates into longer floods and shorter ebbs in the central area of the lagoon. Hence ebb velocities are strongest, which promotes the flushing of sediments seaward. This pattern is enhanced with the increase of the flooded area.

Model results reveal that the increase of the lagoon area as well as the increase of the flooded area depth enhances the tidal prism in all the lagoon channels, but this enhancement is larger in the channels surrounding the flooded area.

In summary, the results suggest that the increase of the flooded area of the lagoon, due to the salt pan walls collapse, could increase the tidal prism and ebb currents enhancing the ebb dominance of the central area, hence contributing to more water exchanges between the lagoon and the sea, improved water quality in the lagoon, and mitigating accretion. Furthermore, the increase of the tidal currents near the inlet will promote the erosion of the main channel, thereby further increasing the tidal prism. This growth of the tidal prism will further reduce the residence times and reduce dredging effort in the main channel due to the accretion currently observed. Hence, the hydrodynamic effects of the collapse of the salt pan walls seem to be generally beneficial for the lagoon.

The risk of flood in coastal systems, as a result of degradation, land reclamation, sea level rise, dredging and/or erosion is a persistent global problem. Thus, the conclusions achieved for the Ria de Aveiro could be generalized to other similar systems at risk of flooding. The outcome of this study indicates that geomorphologic modifications resulted from an enlargement of the flooded area of estuarine systems will induce local tidal changes, with an intensification of the original asymmetry patterns and higher tidal currents and tidal prisms.

Acknowledgements

This work was supported by the Portuguese Science Foundation (FCT) through MURANO (PTDC/ECM/65589/2006), AdaptaRia (PTDC/AAC-CLI/100953/2008) and DyEPlume (PTDC/MAR/107939/2008) Research Projects, co-funded by COMPETE/QREN/UE. The authors thank Profs. Y. Zhang and A.M. Baptista for the model ELCIRC (www.stccmop.org/CORIE/modeling/elcirc).

References

Alves, F., Roebeling, P., Pinto, P., Baptista, P., 2009. Valuing ecosystem service losses from coastal erosion using a benefits transfer approach: a case study for the central Portuguese coast. Journal of Coastal Research, SI 56 (Proceedings of the 10th International Coastal Symposium, Lisbon, Portugal), 1169–1173 ISSN 0749-0258.

Araújo, I.G.B., 2005. Sea level variability: examples from the Atlantic coast of Europe. Ph.D. Thesis, School of the National Oceanography Centre, Southampton, UK.

Araújo, I.G.B., Dias, J.M., Pugh, D.T., 2008. Model simulations of tidal changes in a coastal lagoon, the Ria de Aveiro (Portugal). Continental Shelf Research 28, 1010–1025.

Casulli, V., Cattani, E., 1994. Stability, accuracy and efficiency of a semi-implicit method for 3D shallow water flow. Computers and Mathematics with Applications 27, 99–112.

Crisman, T.L., Takavakoglou, V., Alexandris, T., Antonopoulos, V., Zaladis, G., 2009. Rehabilitation of abandoned saltworks to maximize conservation, ecotourism and water treatment potential. Global Nest Journal 11 (1), 24–31.

da Silva, J.F., Duck, R.W., 2001. Historical changes of bottom topography and tidal amplitude in the Ria de Aveiro, Portugal—trends for future evolution. Climate Research 18, 17–24.

Dias, J.M., 2001. Contribution to the study of the Ria de Aveiro hydrodynamics. Ph.D. Thesis, Universidade de Aveiro, Portugal, 288 pp.

Dias, J.M., Fernandes, E.H., 2006. Tidal and subtidal propagation in two Atlantic estuaries: Patos Lagoon (Brazil) and Ria de Aveiro Lagoon (Portugal). Journal of Coastal Research, SI 39 (Proceedings of the Eighth International Coastal Symposium, Itajaí, SC, Brazil), 1422–1426.

Dias, J.M., Lopes, J.F., 2006a. Implementation and assessment of hydrodynamic, salt and heat transport models: the case of Ria de Aveiro lagoon (Portugal). Environmental Modelling and Software 21, 1–15.

Dias, J.M., Lopes, J.F., 2006b. Calibration and validation of hydrodynamic, salt and heat transport models for Ria de Aveiro lagoon (Portugal). Journal of Coastal Research SI39, 1680–1684.

Dias, J.M., Lopes, J.F., Dekeyser, I., 1999. Hydrological characterization of Ria de Aveiro, Portugal, in early summer. Oceanologica Acta 22 (5), 473–485.

Dias, J.M., Lopes, J.F., Dekeyser, I., 2000. Tidal propagation in Ria de Aveiro lagoon, Portugal. Physics and Chemistry of the Earth (B) 25, 369–374.

Dias, J.M., Sousa, M.C., Bertin, X., Fortunato, A.B., Oliveira, A., 2009. Numerical modeling of the impact of the Ancão Inlet relocation (Ria Formosa, Portugal). Environmental Modelling and Software 24 (2009), 711–725.

Fortunato, A.B., Oliveira, A., Baptista, A.M., 1999. On the effect of tidal flats on the hydrodynamics of the Tagus estuary. Oceanologica Acta 22 (1), 31–44.

Fortunato, A.B., Pinto, L., Oliveira, A., Ferreira, J.S., 2002a. Tidally generated shelf waves off the western Iberian coast. Continental Shelf Research 22 (14), 1935–1950.

Fortunato, A.B., Oliveira, A., Alves, E., 2002b. A study of circulation and salinity intrusion in the Guadiana estuary (Portugal/Spain). Thalassas 18 (2), 43–65.

Fortunato, A.B., Oliveira, A., 2005. Influence on intertidal flats on tidal asymmetry. Journal of Coastal Research 21 (5), 1062–1067.

Friedrichs, C.T., Aubrey, D.G., 1988. Non-linear tidal distortion in shallow well-mixed estuaries: a synthesis. Estuarine, Coastal and Shelf Science 27, 521–545.

Harvey, N., 1988. Coastal management issues for the mouth of the River Murray, SA. Coastal Management 16, 139–149.

INTERREG III B, 2008. Projecto SAL—Sal do Atlântico. Acção6b—Protótipo de recuperação dos muros das marinhas. Relatório Final.

Lopes, J.F., Dias, J.M., Dekeyser, I., 2006. Numerical modelling of cohesive sediments transport in the Ria de Aveiro lagoon, Portugal. Journal of Hydrology 319, 176–198.

Malhadas, S.M., Silva, A., Leitão, P.C., Neves, R., 2009. Effect of the bathymetric changes on the hydrodynamic and residence time in Óbidos Lagoon (Portugal). Journal of Coastal Research, SI 56 (Proceedings of the 10th International Coastal Symposium), 549–553.

Moreira, M.H., Queiroga, H., Machado, M.M., Cunha, M.R., 1993. Environmental gradients in a southern estuarine system: Ria de Aveiro, Portugal, implication for a soft bottom macrofauna colonization. Netherlands Journal of Aquatic Ecology 27 (2–4), 465–482.

Oliveira, A., Fortunato, A.B., Dias, J.M., 2006a. Numerical modelling of the Aveiro inlet dynamics. In: Smith, J.M. (Ed.), Proceedings of the 30th International Conference on Coastal Enginnering, vol. 4. World Scientific Publishing Co., pp. 3282–3294.

Oliveira, A., Fortunato, A.B., Rego, J.R.L., 2006b. Effect of morphological changes on the hydrodynamics and flushing properties of the Óbidos lagoon (Portugal). Continental Shelf Research 26 (8), 917–942.

Oliveira, A., Fortunato, A.B., Pinto, L., 2006c. Modelling the hydrodynamics and the fate of passive and active organisms in the Guadiana estuary. Estuarine, Coastal and Shelf Science 70 (1-2), 76–84.

Pawlowicz, R., Beardsley, B., Lentz, S., 2002. Classical tidal harmonic analysis including error estimates in MATLAB using T_TIDE, Canada. Computers and Geosciences 28, 929–937.

Plecha, S., Rodrigues, S., Silva, P., Dias, J.M., Oliveira, A., Fortunato, A.B., 2007. Trends of bathymetric variations at a tidal inlet. In: Dohmen-Janssen, M., Hulscher, S. (Eds.), Proceedings of the Fifth IAHR Symposium on River, Coastal and Estuarine Morphodynamics, Enschede, The Netherlands, pp. 19–23, ISBN: 0415453631.

Santos, F., Miranda, P., 2006. Alterações Climáticas em Portugal. Cenários, impactes e medidas de adaptação. Portugal Projecto SIAM II, Gradiva, Lisboa.

Vaz, N., Dias, J.M., 2008. Hydrographic characterization of an estuarine tidal channel. Journal of Marine Systems 70, 168–181.

Warner, J.C., Geyer, W.R., Lerczak, J.A., 2005. Numerical modelling of an estuary: a comprehensive skill assessment, USA. Journal of Geophysical Research 110, C05001.

Zhang, Y., Baptista, A.M., Myers, E., 2004. A cross-scale model for 3D baroclinic circulation in estuary-plume-shelf systems: I. Formulation and skill assessment. Continental Shelf Research 24, 2187–2214.